doi: 10.18323/2782-4039-2024-3-69-6

The influence of 3D printing mode on the chemical composition and structure of 30HGSA steel

Yury G. Kabaldin, Doctor of Sciences (Engineering), Professor,
professor of Chair "Technology and Equipment of Mechanical Engineering"
Maksim S. Anosov*, PhD (Engineering), Associate Professor,
assistant professor of Chair "Technology and Equipment of Mechanical Engineering"
Yuliya S. Mordovina, postgraduate student,
educational process engineer of the Institute of Retraining of Specialists
Mikhail A. Chernigin, postgraduate student,
engineer of Chair "Technology and Equipment of Mechanical Engineering"
R.E. Alekseev Nizhny Novgorod State Technical University, Nizhny Novgorod (Russia)

***E-mail:** anosov.ms@nntu.ru,
anosov-maksim@list.ru

Received 31.07.2023 *Accepted 18.12.2023*

Abstract: The authors carried out the study of the influence of 3D printing modes on the structure and chemical composition of 30HGSA steel (chromansil) samples produced by the method of additive electric arc surfacing. To study the influence of the electric arc surfacing mode on the chemical composition of the steel under study, an optical emission analysis of the samples was carried out. The influence of the surfacing mode on the resulting structure was assessed over the entire height of the deposited walls at magnifications of ×50, ×100, ×200 and ×500. Optical emission analysis identified a change in the material chemical composition associated with the loss of chemical elements. It was found that the degree of loss of C, Cr and Si increases almost linearly and is directly proportional to the surfacing heat input (Q, J/mm). The exact influence of an increase in the surfacing heat input on the Mn content was not found, but a relationship between the degree of its loss and the voltage (U, V) during surfacing of samples was identified. Microstructural studies of all samples did not reveal a large number of systemically formed structural defects characteristic of cast and welded products (pores, shrinkage cavities, etc.), which confirms the high quality of the metal in goods produced by electric arc surfacing. Analysis of micrographs taken in different areas of the samples allowed determining that the metal microstructure does not undergo significant changes under different surfacing modes; the main tendencies in changes in the structure along the height of the sample are preserved. All samples demonstrated the formation of a highly dispersed structure, regardless of the 3D printing parameters. The most favorable metal structure, suitable for subsequent use in the production of goods using additive manufacturing, was recognized as the structure of the sample deposited using mode No. 5 (I=160 A, U=24 V, Q=921.6 J/mm). This mode can be used for further study of the problems of additive electric arc surfacing of 30HGSA steel.

Keywords: 30HGSA steel; additive electric arc surfacing; optical emission analysis; metallographic study; additive manufacturing.

Acknowledgements: The study was supported by the grant of the Russian Science Foundation No. 22-79-00095 "Development of scientific and technological foundations for the structure formation of structural materials obtained by additive electric arc growth for the formation of mechanical properties under fatigue using artificial intelligence approaches", https://www.rscf.ru/project/22-79-00095/.

For citation: Kabaldin Yu.G., Anosov M.S., Mordovina Yu.S., Chernigin M.A. The influence of 3D printing mode on the chemical composition and structure of 30HGSA steel. *Frontier Materials & Technologies*, 2024, no. 3, pp. 63–73. DOI: 10.18323/2782-4039-2024-3-69-6.

INTRODUCTION

The intensive development of 3D printing (additive manufacturing) technologies, leads to the necessity of a thorough study of the mechanical properties, structure and chemical composition of metals produced by this method. Today, the main methods of 3D metal printing are layer-by-layer powder melting (Selective Laser Melting, SLM), laser powder surfacing (Laser Engineered Net Shape, LENS / Direct Metal Deposition, DMD) and electric arc surfacing (Wire and Arc Additive Manufacturing, WAAM) [1]. The most technologically productive, and simplest is the method of 3D printing by WAAM, used in this work [2; 3].

The advantages of additive methods include, the ability to automate fully the process of producing goods; a significant reduction in material consumption when manufacturing products from expensive materials, such as titanium and nickel alloys; the possibility of small-scale production of goods, which is unprofitable when using traditional production methods [4–6].

Despite the noted advantages of additive manufacturing methods, the application of these technologies faces

a number of difficulties due to the complexity of selecting printing modes, and thermal cycle parameters. Depending on the selected 3D printing mode, it is possible to obtain different mechanical properties of the material.

SLM is a technology for manufacturing complex products by laser melting of metal powder, using mathematical CAD models. SLM is considered a high-energy process. At the point where the powder melts, the energy density is higher compared to other electric arc processes (for example, welding), but lower than with laser irradiation [7]. One of the problems of SLM-produced parts is the relatively high surface roughness, which reduces fatigue resistance by increasing the stress concentration on the sample surface [8].

Laser powder surfacing (LENS/DMD) is an additive technology for growing a part by fusing a powder material layer onto a substrate. The laser beam creates a welding pool, into which the metal in powder form is injected, where it melts and solidifies to form a metallic bond to the substrate. Typically, this process uses a single-mode continuous wave solid-state fiber laser, operating at a wavelength of 1075 nm. During the process, metal powder from the feed system is automatically fed to the substrate, which is lowered to a height equal to the deposited layer thickness. However, it is noted that the laser surfacing method does not have the reproducibility of the chemical composition, and mechanical properties of the final products [9; 10], which is a serious shortcoming.

WAAM is a relatively new technology emerged in the 1990s. It consists of fusing conventional welding wire widely available commercially onto a substrate, which results in the finished part formation. Compared to conventional manufacturing, WAAM allows reducing production time by 40–60 % and post-processing time by 15–20 %, depending on part size. Thus, aircraft landing gear stiffeners using this technology are manufactured with raw material savings of approximately 78 % compared to conventional production [11]. Metals with good weldability can potentially be used for the WAAM process, and so far, researchers have successfully produced objects from the alloys based on Ti [11], Al [12], steel [13], and Ni [14] using this method.

Stainless low carbon steels (austenitic, martensitic and duplex) are the most preferred candidates for WAAM surfacing due to their combination of mechanical properties, high corrosion resistance and weldability. However, this cannot be said about medium-carbon steels widely used in mechanical engineering, aircraft manufacturing and other fields. Therefore, the study of the behavior of medium-carbon steels during the WAAM process with the prospect of using the developments in industry is of interest.

During the process of surfacing layers, the metal is in a liquid state and is then subjected to multiple heating cycles to temperatures above critical, which leads to a possible change in the chemical composition of the starting material. As a result of non-equilibrium crystallization and repeated heating of the metal, the microstructure of the resulting material differs significantly from the structure of the material obtained from rolled products [15–17].

Foreign research is increasingly considering additive technologies, including WAAM. At the same time, in Russia, these methods are studied locally and are not so widespread. However, it is the use of additive technologies that can reduce the cost of single and small-scale production of goods from widely used structural materials, such as 30HGSA steel. The development of these technologies will contribute to the development of Russian science and import substitution.

The purpose of this research is to study the influence of additive electric arc surfacing modes on the chemical composition and microstructure of 30HGSA steel.

METHODS

The research material was 30HGSA structural steel (GOST 4543-2016 "Rolled Products Made of Alloy Structural Steel. Technical Specifications"). Table 1 presents the grade chemical composition of the deposited 30HGSA steel.

Samples for studying the chemical composition and microstructure of the deposited metal were prepared on a specialized stand for additive electric arc surfacing [18]. Nine blanks in the form of walls (Fig. 1) were produced using various printing modes. The width of the deposited walls was 1 surfacing bead, the height of the walls was formed by depositing 10 layers. A drop of metal was transferred by short circuits.

The surfacing mode was specified by the following parameters: current (I, A), voltage (U, V), arc gap (z, mm), wire feed speed (V, mm/s), and shielding gas consumption. In this case, the arc gap, wire feed speed and shielding gas consumption were constant for all experiments, and amounted to 11 mm and 200 mm/min, respectively (determined by preliminary tests) [19; 20].

Based on the 3D printing modes, the heat input (Q) of the process (electrical energy consumed per length unit of the seam) was determined as one of the complex informative parameters, in accordance with GOST R ISO 857-1-2009, taking into account the energy loss coefficient of 0.8:

Table 1. *Chemical composition of the 30HGSA steel (GOST 4543-2016)*
Таблица 1. *Химический состав стали 30ХГСА (ГОСТ 4543-2016)*

Element	C	Si	Mn	Cr	S	P
Content, %	0.28–0.34	0.90–1.20	0.80–1.10	0.80–1.10	<0.025	<0.025

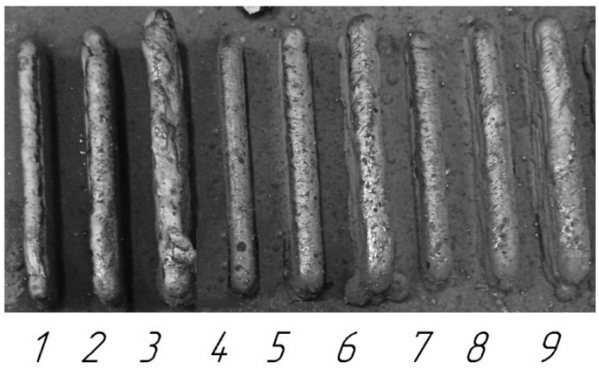

Fig. 1. *General view of the deposited walls*
Рис. 1. *Общий вид наплавленных стенок*

$$Q = \frac{0{,}8\, I\, U}{V}.$$

Table 2 shows the surfacing modes for each welded blank, and the values of the heat input of the surfacing process.

Samples were cut from a wall deposited using the WAAM method across the direction of deposition to study changes in the structure and hardness along the height of the grown metal.

The material chemical composition was determined by emission spectral analysis on a Foundry-Master stationary optical emission analyzer – a high-precision laboratory multi-matrix analyzer with a sensitivity range for most elements of 0.001 % (according to some data, up to 0.0001 %).

The metal microstructure was studied on microsections using an Altami MET 1C optical microscope at magnifications of ×50, ×100, ×200, and ×500. Sample preparation was carried out according to standard technique (mechanical grinding with sandpaper of different grain sizes and polishing using various pastes). Etching was carried out with a 4 % aqueous solution of nitric acid [21].

RESULTS

During the study of the chemical composition of the samples, data reflected in the diagram (Fig. 2) were obtained. The original wire was sample No. 0 shown in Fig. 2. The content of other chemical elements acting as impurities is constant in all studied samples, so these elements are not shown in Fig. 2.

During the study of the microstructure of the samples, practically no technological defects were identified. Large single defects were found only on samples manufactured using modes No. 3 and 7 (Fig. 3).

To compare the quality of different surfacing modes, the microstructure was studied in different regions along the height of the deposited wall of the samples (Fig. 4).

The main microstructural changes are presented in Fig 5–7, and correspond to samples melted using modes No. 1, 5 and 9, respectively, since they allow assessing the main changes in the height of the deposited metal most completely.

In sample No. 1, the wall microstructure near the substrate consists of tempered bainite (Fig. 5 a). In the center of the sample, the bainite structure is generally preserved, but the appearance of other structural components (troostite) is visible. At the top of the sample, the microstructure changes, and consists predominantly of troostosorbite (Fig. 5 c), while the columnarity of the grains caused by the temperature gradient during cooling of the deposited bead is partially retained. Clearly defined ferrite grains are observed. One should note that the last deposited layers of sample No. 1 are characterized by a rather high degree of grain size nonhomogeneity.

The microstructure of sample No. 5 near the substrate is also represented by tempered bainite (Fig. 6 a). In this sample, the tendency for a uniform transition from the bainite structure to the troostosorbite structure

Table 2. *Deposition modes for each blank produced by the WAAM method*
Таблица 2. *Режимы наплавки для каждой заготовки, полученной методом WAAM*

Blank No.	**1**	**2**	**3**	**4**	**5**	**6**	**7**	**8**	**9**
***I*, A**	120	160	200	120	160	200	120	160	200
***U*, B**	18	18	18	24	24	24	27	27	27
***Q*, J/mm**	518.4	691.2	864.0	691.2	921.6	1,152.0	777.6	1,036.8	1,296.0

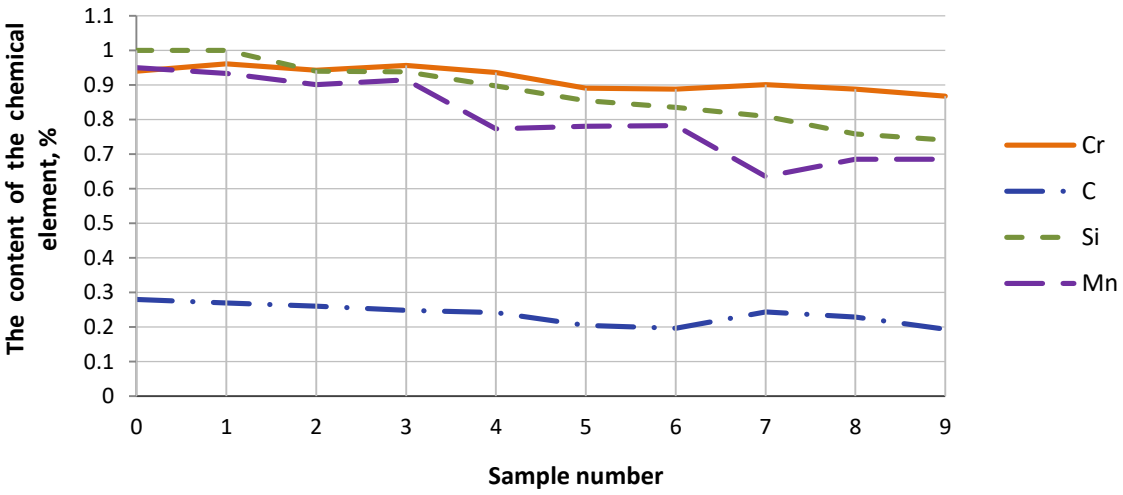

Fig. 2. *Change in the content of alloying elements depending on the deposition mode*
Рис. 2. *Изменение содержания легирующих элементов в зависимости от режима наплавки*

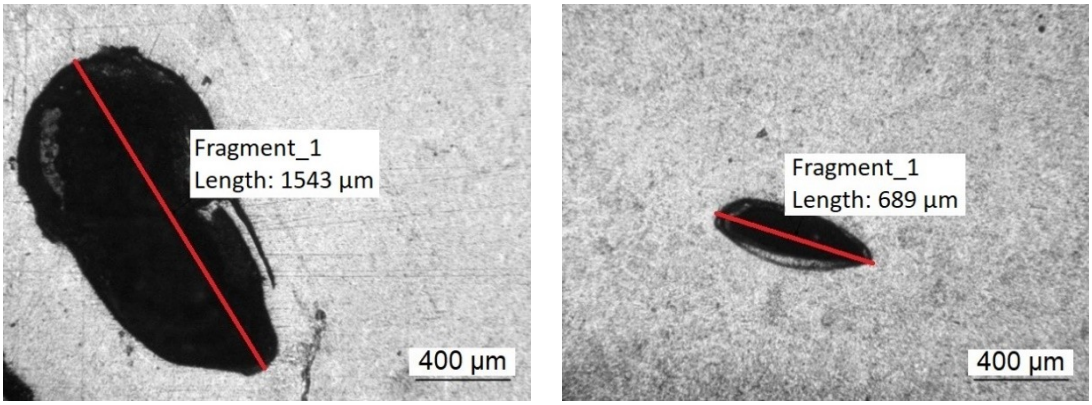

a ***b***

Fig. 3. *Defects identified in the structure of samples, ×50:*
a *– sample No. 3;* ***b*** *– sample No. 7*
Рис. 3. *Дефекты, выявленные в структуре образцов, ×50:*
a *– образец № 3;* ***b*** *– образец № 7*

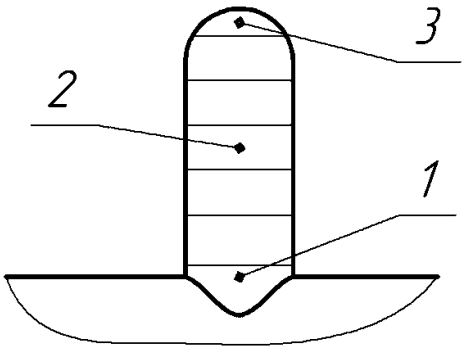

Fig. 4. *Location of characteristic zones for studying the microstructure of the sample:*
1 – base; 2 – center; 3 – top
Рис. 4. *Расположение характерных зон для исследования микроструктуры образца:*
1 – основание; 2 – центр; 3 – вершина

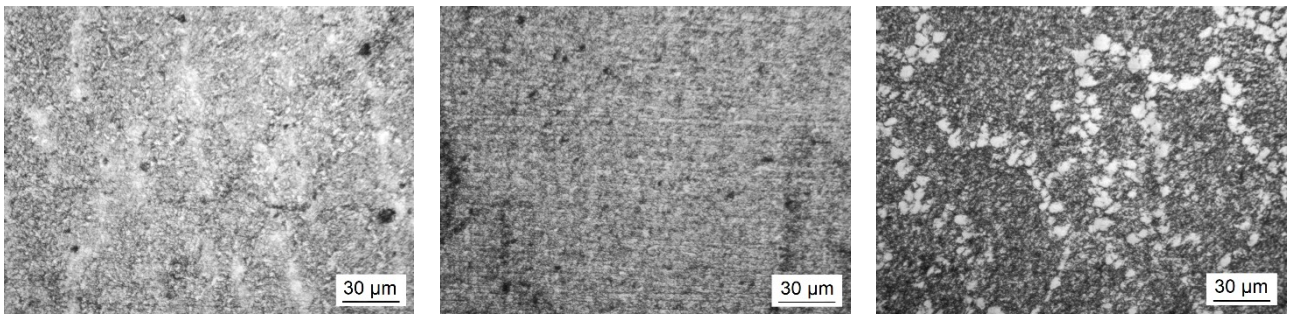

a ***b*** ***c***

Fig. 5. *Microstructure of the deposited wall (30HGSA steel, sample No. 1, Q=518.4 J/mm) (×500):*
a *– near the substrate;* ***b*** *– in the center of the sample;* ***c*** *– at the top of the sample*
Рис. 5. *Микроструктура наплавленной стенки (сталь 30ХГСА, образец № 1, Q=518,4 Дж/мм) (×500):*
a *– вблизи подложки;* ***b*** *– в центре образца;* ***c*** *– в вершине образца*

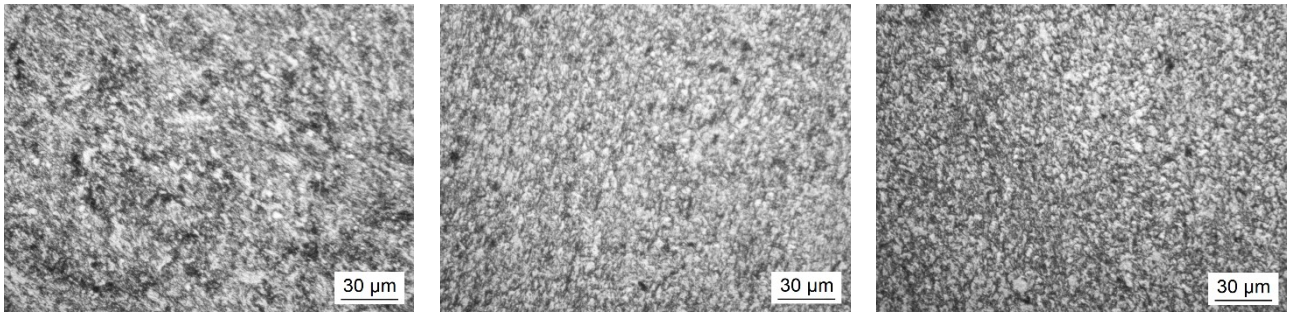

a ***b*** ***c***

Fig. 6. *Microstructure of the deposited wall (30HGSA steel, sample No. 5, Q=921.6 J/mm) (×500):*
a *– near the substrate;* ***b*** *– in the center of the sample;* ***c*** *– at the top of the sample*
Рис. 6. *Микроструктура наплавленной стенки (сталь 30ХГСА, образец № 5, Q=921,6 Дж/мм) (×500):*
a *– вблизи подложки;* ***b*** *– в центре образца;* ***c*** *– в вершине образца*

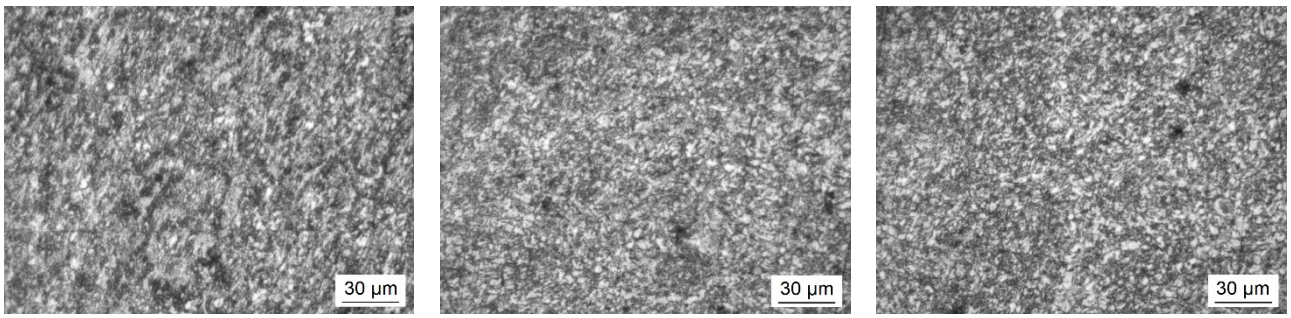

a ***b*** ***c***

Fig. 7. *Microstructure of the deposited wall (30HGSA steel, sample No. 9, Q=1296 J/mm) (×500):*
a *– near the substrate;* ***b*** *– in the center of the sample;* ***c*** *– at the top of the sample*
Рис. 7. *Микроструктура наплавленной стенки (сталь 30ХГСА, образец № 9, Q=1296 Дж/мм) (×500):*
a *– вблизи подложки;* ***b*** *– в центре образца;* ***c*** *– в вершине образца*

remains, but the structure change proceeds more smoothly. The microstructure of all areas does not reveal grain size nonhomogeneity, and grain columnarity in the last surfacing beads.

The microstructure of sample No. 9 near the surfacing, mainly consists of tempered bainite (Fig. 7 a). One should note that with this surfacing mode, inclusions of other structural components (troostosorbite), are visible in the main bainite structure. This sample also retains the tendency of a gradual transition from the bainite structure to the troostosorbite structure, but it is represented by larger grains. In general, the microstructure of the sample deposited using mode No. 9 is coarser than the structure of the other samples.

In samples No. 1–3, an area with a sharp change in the structure relating to the last 2–3 layers of surfacing was identified (Fig. 8).

The study of micrographs of different samples did not reveal a large number of structural defects characteristic of cast and welded products (pores, shrinkage cavities, etc.). One should note that a highly dispersed structure was obtained for all surfacing modes.

DISCUSSION

Based on the results of spectral analysis, the authors found that when manufacturing products using 3D metal printing technology, there is a decrease in the content of carbon and main alloying elements, such as Si, Mn and Cr. This phenomenon actively manifests itself during welding and casting of metals, and is associated with the material liquid state. Technologically, the process of 3D metal printing is similar to welding; therefore, a change in the content of chemical elements is a loss of metal.

It was found that the C, Si and Cr content decreases almost linearly. One can note that when increasing the heat input of the surfacing process, the proportion of loss increases. The influence of the heat input of surfacing on the Mn content is not so clear. It was found that the loss of Mn is the same for samples deposited with the same voltage. The decrease in Mn content occurs in steps and corresponds to a voltage increase during surfacing.

Microstructural analysis revealed virtually no defects characteristic of cast or welded products (pores, shrinkage cavities, etc.) [22]. Large single defects (shrinkage cavities) were detected only in samples manufactured according to modes No. 3 and 7 (Fig. 3). The above defects were not detected in samples made using other surfacing modes.

When studying other sections of samples No. 3 and 7, defects were not re-identified, which may indicate the non-systemic nature of the formation of shrinkage cavities in the samples. One can conclude that the occurrence of cavities is not related to the surfacing mode, and is caused by a single violation of the surfacing technology.

Summarizing the microstructural analysis data, one can identify zoning in the deposited material depending on the order of the deposited layer, with the zones smoothly transitioning from one to another (except for samples No. 1–3). Thus, near the substrate, the structure is represented by tempered bainite. The occurrence of this structure is caused by a rather high cooling temperature after surfacing, and the supply of sufficient heat energy during surfacing of subsequent layers. The microstructure of the middle deposited layers of 30HGSA steel, in addition to bainite, contained troostite, which can be explained by the slower cooling of this area, during which the S-curve nose was affected (Fig. 5 b). The energy supplied after surfacing is also sufficient for tempering processes to occur. According to mode No. 5, the most homogeneous microstructure is formed, which should ensure isotropy of properties.

In the last deposited layers, troostosorbite is detected, but in sample No. 1, grain size nonhomogeneity with a sharp zone transition is observed (Fig. 8), which may be associated with the shorter time when the metal of these areas is at temperatures close to critical; sample No. 9 has coarse grains with columnar crystals. These shortcomings lead to a decrease in strength properties, and unsatisfactory results during subsequent heat treatment.

Unlike samples No. 1 and 9, these defects were not found in the upper layers of sample No. 5. Consequently, even without heat treatment, this structure is more efficient, and further heat treatment according to the correct mode will only improve the properties of the deposited 30HGSA metal.

The described differences in the microstructure of the samples are explained by the heat input during

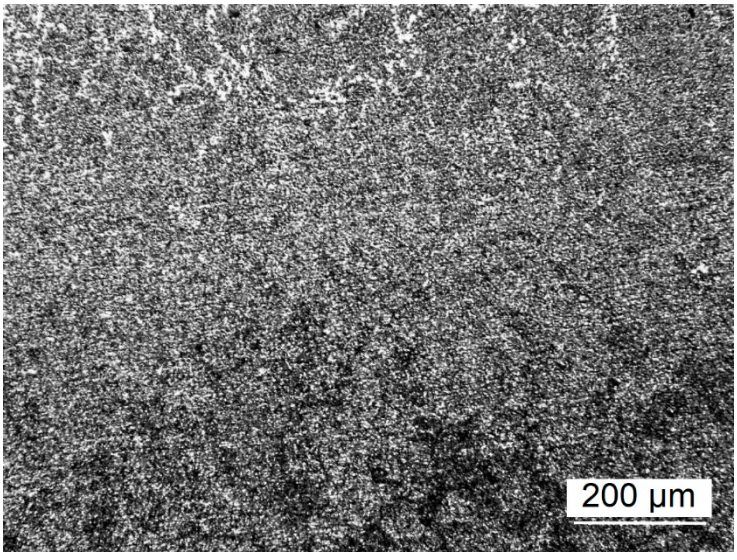

Fig. 8. *Example of an area with a sharp change in the structure, ×100*
Рис. 8. *Пример области с резким изменением структуры, ×100*

surfacing, and the cooling rate. Due to the relatively small heat input (compared to other modes), sample No. 1 has a lower cooling rate, which facilitates the phase transformation of steel, through the diffusion mechanism. Therefore, troostite and ferrite grains appear in the microstructure (Fig. 5 c).

For sample No. 5, the amount of heat input during the surfacing process is optimal, so the temperature gradient between the metal and the environment is sufficient, so that after surfacing, the 30HGSA steel cools at the rate necessary for the formation of highly dispersed bainite. A similar bainitic structure in the 30HGSA steel is formed during the fabrication of welds [23].

The heat input of surfacing for sample No. 9 promotes the bainite formation; however, a large amount of heat input provokes grain growth, which makes the structure of the upper layers coarser.

Pores of various sizes were observed in the deposited samples (Fig. 3), and this fact raises the question of the permissible porosity level. The same question arose in [24] in relation to SLM technology, which is related to WAAM technology. As the authors note, controlling the energy density in limited areas of the SLM process currently used for porosity prediction is insufficient considering the complexity of the process. This statement is also applicable to WAAM.

Thus, the 30HGSA steel microstructure has zones whose structural composition does not depend on the surfacing mode, but the surfacing mode affects the structure dispersion and defectiveness. Different results were obtained for 09G2S and 06H19N9T steels [25]. Obtaining results different from those described above may be caused by different weldability of the steel grades under consideration. 30HGSA steel, unlike 09G2S and 06H19N9T steels, is partially weldable. The presence of zoning along the height of the deposited metal was also observed in titanium alloys [26].

Microstructural analysis of samples produced under different surfacing modes identified that the most favorable metal structure is the structure of sample No. 5 (I=160 A, U=24 V, Q=921.6 J/mm), which gives grounds to use it as a working material for further research.

It is necessary as well to carry out additional work to demonstrate the corrosion resistance of samples produced by the WAAM method. In paper [27], using the example of corrosion-resistant SS 316 steel, it is shown that samples produced by the WAAM method have higher corrosion resistance than samples produced by sand casting. At the same time, the lower deposited layers of the WAAM samples had lower corrosion resistance than the upper ones, which is associated with the difference in heat input. Taking into account the non-homogeneity of the 30HGSA steel microstructure along the height of the deposited wall, one should also expect a scatter in the corrosion properties in this section.

However, in [28], the opposite is shown using the example of magnesium alloys. The authors tried to obtain a magnesium alloy using WAAM technology with the prospect of using it in biomedicine. However, at this stage of technology development, this is impossible due to the reduced corrosion resistance, and biocompatibility of magnesium alloys produced by the WAAM method. Similar problems are observed for steels.

The work [29] raises the problems of certification of WAAM products, and non-destructive testing. This is a labor-intensive task, since initially it is necessary to remove the WAAM surfacing method from the category of research ones, and used mainly for single production. Only after this, it will be possible to talk about the development of standards that will allow evaluating correctly, the properties of manufactured products.

CONCLUSIONS

1. When surfacing products using various surfacing modes, a change in the material chemical composition is observed, associated with the loss of chemical elements. The degree of loss of C, Cr and Si increases with increasing heat input of the layer surfacing (Q) and changes almost linearly. Mn loss depends on the 3D printing voltage.

2. The metal microstructure does not undergo significant changes when the surfacing mode changes. The main tendencies in the change in the structure along the sample height are preserved: a gradual transition from a bainite structure near the substrate to a troostosorbite structure corresponding to the last surfacing beads, is observed.

3. For all samples, a large number of systemically formed structural defects characteristic of cast and welded products (pores, shrinkage cavities, etc.) was not identified. One should note that a highly dispersed structure was obtained in all samples, regardless of the 3D printing parameters. The exception is the sample deposited using mode No. 9 (I=200 A, U=27 V, Q=1296 J/mm): in this case, the resulting structure was characterized by a larger grain size than the structure of the other samples.

4. The structure of sample No. 5 (I=160 A, U=24 V, Q=921.6 J/mm) was recognized as the most favorable metal structure suitable for subsequent use in the production of goods using 3D printing.

REFERENCES

1. Li Johnnie Liew Zhong, Alkahari M.R., Rosli N.A.B., Hasan R., Sudin M.N., Ramli F.R. Review of Wire Arc Additive Manufacturing for 3D Metal Printing. *International Journal of Automation Technology*, 2019, vol. 13, no. 3, pp. 346–353. DOI: 10.20965/ijat.2019.p0346.
2. Ding Donghong, Pan Zengxi, Cuiuri D., Li Huijun. Wire-feed additive manufacturing of metal components: technologies, developments and future interests. *The International Journal of Advanced Manufacturing Technology*, 2015, vol. 81, pp. 465–481. DOI: 10.1007/s00170-015-7077-3.
3. Wu Bintao, Pan Zengxi, Ding Donghong, Cuiuri D., Li Huijun, Xu Jing, Norrish J. A review of the wire arc additive manufacturing of metals: Properties, defects and quality improvement. *Journal of Manufacturing Processes*, 2018, vol. 35, pp. 127–139. DOI: 10.1016/j.jmapro.2018.08.001.
4. Oskolkov A.A., Matveev E.V., Bezukladnikov I.I., Trushnikov D.N., Krotova E.L. Advanced technologies for additive manufacturing of metal product. *Bulletin of*

Perm national research polytechnic university. Mechanical engineering, materials science, 2018, vol. 20, no. 3, pp. 90–105. DOI: 10.15593/2224-9877/2018.3.11.

5. Cunningham C.R., Wikshåland S., Xu F., Kemakolam N., Shokrani A., Dhokia V., Newman S.T. Cost modelling and sensitivity analysis of wire and arc additive manufacturing. *Procedia Manufacturing*, 2017, vol. 11, pp. 650–657. DOI: 10.1016/j.promfg.2017.07.163.
6. Pant H., Arora A., Gopakumar G.S., Chadha U., Saeidi A., Patterson A.E. Applications of wire arc additive manufacturing (WAAM) for aerospace component manufacturing. *The International Journal of Advanced Manufacturing Technology*, 2023, vol. 127, pp. 4995–5011. DOI: 10.1007/s00170-023-11623-7.
7. Wang Fude, Williams S., Rush M. Morphology investigation on direct current pulsed gas tungsten arc welded additive layer manufactured Ti6Al4V alloy. *The International Journal of Advanced Manufacturing Technology*, 2011, vol. 57, pp. 597–603. DOI: 10.1007/s00170-011-3299-1.
8. Ahmadkhaniha D., Möller H., Zanella C. Studying the Microstructural Effect of Selective Laser Melting and Electropolishing on the Performance of Maraging Steel. *Journal of Materials Engineering and Performance*, 2021, vol. 30, pp. 6588–6605. DOI: 10.1007/s11665-021-05927-6.
9. Beese A.M., Carroll B.E. Review of mechanical properties of Ti–6Al–4V made by laser-based additive manufacturing using powder feedstock. *JOM*, 2016, vol. 68, pp. 724–734. DOI: 10.1007/s11837-015-1759-z.
10. Kirka M.M., Lee Y., Greeley D.A., Okello A., Goin M.J., Pearce M.T., Dehoff R.R. Strategy for texture management in metals additive manufacturing. *JOM*, 2017, vol. 69, pp. 523–531. DOI: 10.1007/s11837-017-2264-3.
11. Williams S.W., Martina F., Addison A.C., Ding J., Pardal G., Colegrove P. Wire + arc additive manufacturing. *Materials Science and Technology*, 2016, vol. 32, no. 7, pp. 641–647. DOI: 10.1179/1743284715Y.0000000073.
12. Gu Jianglong, Ding Jialuo, Williams S.W., Gu Huimin, Bai Jing, Zhai Yuchun, Ma Peihua. The strengthening effect of inter-layer cold working and post-deposition heat treatment on the additively manufactured Al–6.3Cu alloy. *Materials Science and Engineering: A*, 2016, vol. 651, pp. 18–26. DOI: 10.1016/j.msea.2015.10.101.
13. Guo Nannan, Leu Ming. Additive manufacturing: Technology, applications and research needs. *Frontiers of Mechanical Engineering*, 2013, vol. 8, pp. 215–243. DOI: 10.1007/s11465-013-0248-8.
14. Xu Fujia, Lv Yaohui, Liu Yuxin, Shu Fengyuan, He Peng, Xu Binshi. Microstructural Evolution and Mechanical Properties of Inconel 625 Alloy during Pulsed Plasma Arc Deposition Process. *Journal of Material Science and Technology*, 2013, vol. 29, no. 5, pp. 480–488. DOI: 10.1016/j.jmst.2013.02.010.
15. Kudryashov V.A., Lapyshev A.A. The creation of additive technologies taking into account the fatigue behaviour of a material in aviation engineering. *Izvestiya of Samara Scientific Center of the Russian Academy of Sciences*, 2018, vol. 20, no. 4-3, pp. 406–413. EDN: YVOALR.
16. Kubanova A.N., Sergeev A.N., Dobrovolskiy N.M., Gvozdev A.E., Medvedev P.N., Maliy D.V. Materials and technologies for production products by additive manufacturing. *Chebyshevskii sbornik*, 2019, vol. 20, no. 3, pp. 453–477. DOI: 10.22405/2226-8383-2019-20-3-453-477.
17. Terentev V.F., Korableva S.A. *Ustalost metallov* [Fatigue of metals]. Moscow, Nauka Publ., 2015. 484 p.
18. Kabaldin Yu.G., Shatagin D.A., Anosov M.S., Kolchin P.V., Kiselev A.V. Diagnostics of 3D printing on a CNC machine by machine learning. *Russian engineering research*, 2021, vol. 41, no. 4, pp. 320–324. DOI: 10.3103/S1068798X21040109.
19. Atroshchenko V.V., Tefanov V.N., Kraev K.A. Revisited the control of metal transfer during welding by consumable electrode with a short circuit of arc interval. *Vestnik USATU*, 2008, vol. 11, no. 2, pp. 146–154. EDN: JXECOH.
20. Anosov M.C., Shatagin D.A., Chernigin M.A., Mordovina Yu.S., Anosova E.S. Structure formation of Np-30KHGSA alloy in wire and arc additive manufacturing. *Izvestiya. Ferrous Metallurgy (Izvestiya vuzov. Chernaya Metallurgiya)*, 2023, vol. 66, no. 3, pp. 294–301. DOI: 10.17073/0368-0797-2023-3-294-301.
21. Jovičević-Klug P., Lipovšek N., Jovičević-Klug M., Podgornik B. Optimized Preparation of Deep Cryogenic Treated Steel and Al-alloy Samples for Optimal Microstructure Imaging Results. *Materials Today Communications*, 2021, vol. 27, article number 102211. DOI: 10.1016/j.mtcomm.2021.102211.
22. Rybakov A.A., Filipchuk T.N., Demchenko Yu.V. Optimization of the chemical composition and structure of the metal of repair welds when fixing defects in welded pipe joints using multilayer welding. *The Paton Welding Journal*, 2013, no. 12, pp. 24–30. EDN: SYLXOT.
23. Chinakhov D.A., Skakov M.K., Gradoboev A.V., Uvaliev B.K., Sharov V.V. Change of microstructure and mechanical properties of multilayered connections from steel 30XGSA at fusion welding using different methods. *Bulletin of the Tomsk Polytechnic University. Geo Assets Engineering*, 2008, vol. 313, no. 2, pp. 119–122. EDN: JVJFVT.
24. Balyakin A.V., Zhuchenko E.I., Smirnov G.V., Pronichev N.D. The investigation of negative technological heredity appearance during GTE parts manufacturing by SLM method. *Izvestiya of Samara Scientific Center of the Russian Academy of Sciences*, 2019, vol. 21, no. 1, pp. 61–70. EDN: XHSWIU.
25. Zhatkin S.S., Nikitin K.V., Deev V.B., Pankratov S.S., Dunaev D.A. Application of electric arc surfacing in the manufacturing of three-dimensional steel products. *Izvestiya. Ferrous Metallurgy (Izvestiya vuzov. Chernaya Metallurgiya)*, 2020, vol. 63, no. 6, pp. 443–450. DOI: 10.17073/0368-0797-2020-6-443-450.
26. Wang Fude, Williams S., Colegrove P., Antonysamy A.A. Microstructure and Mechanical Properties of Wire and Arc Additive Manufactured Ti–6Al–4V. *Metallurgical and Materials Transactions A*, 2013, vol. 44, pp. 968–977. DOI: 10.1007/s11661-012-1444-6.
27. Gürol U., Kocaman E., Dilibal S., Koçak M. A comparative study on the microstructure, mechanical properties, wear and corrosion behaviors of SS 316 austenitic stainless steels manufactured by casting and WAAM

technologies. *CIRP Journal of Manufacturing Science and Technology*, 2023, vol. 47, pp. 215–227. DOI: 10.1016/j.cirpj.2023.10.005.
28. Takagi H., Sasahara H., Abe T., Sannomiya H., Nishiyama Sh., Ohta Sh., Nakamura K. Material-property evaluation of magnesium alloys fabricated using wire-and-arc-based additive manufacturing. *Additive Manufacturing*, 2018, vol. 24, pp. 498–507. DOI: 10.1016/J.ADDMA.2018.10.026.
29. Rodrigues T.A., Duarte V., Miranda R.M., Santos T.G., Oliveira J.P. Current Status and Perspectives on Wire and Arc Additive Manufacturing (WAAM). *Materials*, 2019, vol. 12, no. 7, article number 1121. DOI: 10.3390/ma12071121.

СПИСОК ЛИТЕРАТУРЫ

1. Li Johnnie Liew Zhong, Alkahari M.R., Rosli N.A.B., Hasan R., Sudin M.N., Ramli F.R. Review of Wire Arc Additive Manufacturing for 3D Metal Printing // International Journal of Automation Technology. 2019. Vol. 13. № 3. P. 346–353. DOI: 10.20965/ijat.2019.p0346.
2. Ding Donghong, Pan Zengxi, Cuiuri D., Li Huijun. Wire-feed additive manufacturing of metal components: technologies, developments and future interests // The International Journal of Advanced Manufacturing Technology. 2015. Vol. 81. P. 465–481. DOI: 10.1007/s00170-015-7077-3.
3. Wu Bintao, Pan Zengxi, Ding Donghong, Cuiuri D., Li Huijun, Xu Jing, Norrish J. A review of the wire arc additive manufacturing of metals: Properties, defects and quality improvement // Journal of Manufacturing Processes. 2018. Vol. 35. P. 127–139. DOI: 10.1016/j.jmapro.2018.08.001.
4. Осколков А.А., Матвеев Е.В., Безукладников И.И., Трушников Д.Н., Кротова Е.Л. Передовые технологии аддитивного производства металлических изделий // Вестник Пермского национального исследовательского политехнического университета. Машиностроение, материаловедение. 2018. Т. 20. № 3. С. 90–105. DOI: 10.15593/2224-9877/2018.3.11.
5. Cunningham C.R., Wikshåland S., Xu F., Kemakolam N., Shokrani A., Dhokia V., Newman S.T. Cost modelling and sensitivity analysis of wire and arc additive manufacturing // Procedia Manufacturing. 2017. Vol. 11. P. 650–657. DOI: 10.1016/j.promfg.2017.07.163.
6. Pant H., Arora A., Gopakumar G.S., Chadha U., Saeidi A., Patterson A.E. Applications of wire arc additive manufacturing (WAAM) for aerospace component manufacturing // The International Journal of Advanced Manufacturing Technology. 2023. Vol. 127. P. 4995–5011. DOI: 10.1007/s00170-023-11623-7.
7. Wang Fude, Williams S., Rush M. Morphology investigation on direct current pulsed gas tungsten arc welded additive layer manufactured Ti6Al4V alloy // The International Journal of Advanced Manufacturing Technology. 2011. Vol. 57. P. 597–603. DOI: 10.1007/s00170-011-3299-1.
8. Ahmadkhaniha D., Möller H., Zanella C. Studying the Microstructural Effect of Selective Laser Melting and Electropolishing on the Performance of Maraging Steel // Journal of Materials Engineering and Performance. 2021. Vol. 30. P. 6588–6605. DOI: 10.1007/s11665-021-05927-6.
9. Beese A.M., Carroll B.E. Review of mechanical properties of Ti–6Al–4V made by laser-based additive manufacturing using powder feedstock // JOM. 2016. Vol. 68. P. 724–734. DOI: 10.1007/s11837-015-1759-z.
10. Kirka M.M., Lee Y., Greeley D.A., Okello A., Goin M.J., Pearce M.T., Dehoff R.R. Strategy for texture management in metals additive manufacturing // JOM. 2017. Vol. 69. P. 523–531. DOI: 10.1007/s11837-017-2264-3.
11. Williams S.W., Martina F., Addison A.C., Ding J., Pardal G., Colegrove P. Wire + arc additive manufacturing // Materials Science and Technology. 2016. Vol. 32. № 7. P. 641–647. DOI: 10.1179/1743284715Y.0000000073.
12. Gu Jianglong, Ding Jialuo, Williams S.W., Gu Huimin, Bai Jing, Zhai Yuchun, Ma Peihua. The strengthening effect of inter-layer cold working and post-deposition heat treatment on the additively manufactured Al–6.3Cu alloy // Materials Science and Engineering: A. 2016. Vol. 651. P. 18–26. DOI: 10.1016/j.msea.2015.10.101.
13. Guo Nannan, Leu Ming. Additive manufacturing: Technology, applications and research needs // Frontiers of Mechanical Engineering. 2013. Vol. 8. P. 215–243. DOI: 10.1007/s11465-013-0248-8.
14. Xu Fujia, Lv Yaohui, Liu Yuxin, Shu Fengyuan, He Peng, Xu Binshi. Microstructural Evolution and Mechanical Properties of Inconel 625 Alloy during Pulsed Plasma Arc Deposition Process // Journal of Material Science and Technology. 2013. Vol. 29. № 5. P. 480–488. DOI: 10.1016/j.jmst.2013.02.010.
15. Кудряшов В.А., Лапышев А.А. Создание аддитивных технологий с учетом усталостного поведения материала в авиационном инжиниринге // Известия Самарского научного центра Российской академии наук. 2018. Т. 20. № 4-3. С. 406–413. EDN: YVOALR.
16. Кубанова А.Н., Сергеев А.Н., Добровольский Н.М., Гвоздев А.Е., Медведев П.Н., Малий Д.В. Особенности материалов и технологий аддитивного производства изделий // Чебышевский сборник. 2019. Т. 20. № 3. С. 453–477. DOI: 10.22405/2226-8383-2019-20-3-453-477.
17. Терентьев В.Ф., Кораблева С.А. Усталость металлов. М.: Наука, 2015. 484 с.
18. Кабалдин Ю.Г., Шатагин Д.А., Аносов М.С., Колчин П.В., Киселев А.В. Диагностика процесса 3D-печати на станке с ЧПУ с использованием подходов машинного обучения // Вестник машиностроения. 2021. № 1. С. 55–59. DOI: 10.36652/0042-4633-2021-1-55-59.
19. Атрощенко В.В., Тефанов В.Н., Краев К.А. К вопросу об управлении переносом электродного металла при дуговой сварке плавящимся электродом с короткими замыканиями дугового промежутка // Вестник Уфимского государственного авиационного технического университета. 2008. Т. 11. № 2. С. 146–154. EDN: JXECOH.
20. Аносов М.С., Шатагин Д.А., Чернигин М.А., Мордовина Ю.С., Аносова Е.С. Структурообразование сплава Нп-30ХГСА при аддитивном электродуговом

выращивании // Известия высших учебных заведений. Черная металлургия. 2023. Т. 66. № 3. С. 294–301. DOI: 10.17073/0368-0797-2023-3-294-301.
21. Jovičević-Klug P., Lipovšek N., Jovičević-Klug M., Podgornik B. Optimized Preparation of Deep Cryogenic Treated Steel and Al-alloy Samples for Optimal Microstructure Imaging Results // Materials Today Communications. 2021. Vol. 27. Article number 102211. DOI: 10.1016/j.mtcomm.2021.102211.
22. Рыбаков А.А., Филипчук Т.Н., Демченко Ю.В. Оптимизация химического состава и структуры металла ремонтных швов при исправлении дефектов в сварных соединениях труб с применением многослойной сварки // Автоматическая сварка. 2013. № 12. С. 24–30. EDN: SYLXOT.
23. Чинахов Д.А., Скаков М.К., Градобоев А.В., Увалиев Б.К., Шаров В.В. Изменение микроструктуры и механических свойств многослойных соединений из стали 30ХГСА при сварке плавлением разными способами // Известия Томского политехнического университета. Инжиниринг георесурсов. 2008. Т. 313. № 2. С. 119–122. EDN: JVJFVT.
24. Балякин А.В., Жученко Е.И., Смирнов Г.В., Проничев Н.Д. Исследование проблем появления негативной технологической наследственности при изготовлении деталей ГТД методом селективного лазерного сплавления // Известия Самарского научного центра Российской академии наук. 2019. Т. 21. № 1. С. 61–70. EDN: XHSWIU.
25. Жаткин С.С., Никитин К.В., Деев В.Б., Панкратов С.С., Дунаев Д.А. Применение электродуговой наплавки для создания трехмерных объектов из стали // Известия высших учебных заведений. Черная металлургия. 2020. Т. 63. № 6. С. 443–450. DOI: 10.17073/0368-0797-2020-6-443-450.
26. Wang Fude, Williams S., Colegrove P., Antonysamy A.A. Microstructure and Mechanical Properties of Wire and Arc Additive Manufactured Ti–6Al–4V // Metallurgical and Materials Transactions A. 2013. Vol. 44. P. 968–977. DOI: 10.1007/s11661-012-1444-6.
27. Gürol U., Kocaman E., Dilibal S., Koçak M. A comparative study on the microstructure, mechanical properties, wear and corrosion behaviors of SS 316 austenitic stainless steels manufactured by casting and WAAM technologies // CIRP Journal of Manufacturing Science and Technology. 2023. Vol. 47. P. 215–227. DOI: 10.1016/j.cirpj.2023.10.005.
28. Takagi H., Sasahara H., Abe T., Sannomiya H., Nishiyama Sh., Ohta Sh., Nakamura K. Material-property evaluation of magnesium alloys fabricated using wire-and-arc-based additive manufacturing // Additive Manufacturing. 2018. Vol. 24. P. 498–507. DOI: 10.1016/J.ADDMA.2018.10.026.
29. Rodrigues T.A., Duarte V., Miranda R.M., Santos T.G., Oliveira J.P. Current Status and Perspectives on Wire and Arc Additive Manufacturing (WAAM) // Materials. 2019. Vol. 12. № 7. Article number 1121. DOI: 10.3390/ma12071121.

Влияние режима 3D-печати на химический состав и структуру стали 30ХГСА

Кабалдин Юрий Георгиевич, доктор технических наук, профессор,
профессор кафедры «Технология и оборудование машиностроения»
Аносов Максим Сергеевич*, кандидат технических наук, доцент,
доцент кафедры «Технология и оборудование машиностроения»
Мордовина Юлия Сергеевна, аспирант,
инженер по учебному процессу института переподготовки специалистов
Чернигин Михаил Алексеевич, аспирант,
инженер кафедры «Технология и оборудование машиностроения»
Нижегородский государственный технический университет им. Р.Е. Алексеева, Нижний Новгород (Россия)

***E-mail:** anosov.ms@nntu.ru,
anosov-maksim@list.ru

Поступила в редакцию 31.07.2023 *Принята к публикации 18.12.2023*

Аннотация: Проведено исследование влияния режимов 3D-печати на структуру и химический состав образцов из стали 30ХГСА (хромансиль, англ. *chromansil*), полученных методом аддитивной электродуговой наплавки. Для исследования влияния режима электродуговой наплавки на химический состав исследуемой стали проведен оптико-эмиссионный анализ образцов. Оценка влияния режима наплавки на получаемую структуру проводилась по всей высоте наплавленных стенок при увеличениях ×50, ×100, ×200 и ×500. В ходе оптико-эмиссионного анализа выявлено изменение химического состава материала, связанное с угаром химических элементов. Установлено, что степень угара C, Cr и Si растет практически линейно и прямо пропорциональна погонной энергии наплавки (Q, Дж/мм). Точного влияния роста величины погонной энергии наплавки на содержание Mn не установлено, но выявлена взаимосвязь между степенью его угара и напряжением (U, В) при наплавке образцов. В ходе микроструктурных исследований всех образцов не выявлено большого количества системно образовавшихся структурных дефектов, характерных для литых и сварных изделий (поры, усадочные раковины и т. д.), что подтверждает

высокое качество металла в изделиях, полученных методом электродуговой наплавки. Анализ микроснимков, сделанных на различных участках образцов, позволил определить, что микроструктура металла не претерпевает сильных изменений при разных режимах наплавки, сохраняются основные тенденции изменения структуры по высоте образца. На всех образцах отмечено получение высокодисперсной структуры вне зависимости от параметров 3D-печати. Наиболее благоприятной структурой металла, подходящей для последующего использования при производстве изделий методом 3D-печати, признана структура образца, наплавленного по режиму № 5 (I=160 А, U=24 В, Q=921,6 Дж/мм). Данный режим может быть использован для дальнейшего изучения проблем аддитивной электродуговой наплавки стали 30ХГСА.

Ключевые слова: сталь 30ХГСА; аддитивная электродуговая наплавка; оптический эмиссионный анализ; металлографические исследования; 3D-печать.

Благодарности: Исследование выполнено при поддержке гранта Российского научного фонда № 22-79-00095 «Разработка научно-технологических основ структурообразования конструкционных материалов полученных путем аддитивного электродугового выращивания для формирования механических свойств при усталости с использованием подходов искусственного интеллекта», https://www.rscf.ru/project/22-79-00095/.

Для цитирования: Кабалдин Ю.Г., Аносов М.С., Мордовина Ю.С., Чернигин М.А. Влияние режима 3D-печати на химический состав и структуру стали 30ХГСА // Frontier Materials & Technologies. 2024. № 3. С. 63–73. DOI: 10.18323/2782-4039-2024-3-69-6.